

Application of interferometry and holography for precision measurements

Hans J. Tiziani

Institute of Applied Optics, University of Stuttgart
Pfaffenwaldring 9, 7000 Stuttgart 80, FRG

Abstract

Phase measurement techniques are becoming a useful tool for precision measurements. Spatial as well as temporal phase shift methods can be used. Optical testing, where computer analysis of interference fringes is becoming increasingly important, will be discussed in connection with testing optical components, microprofiles as well as for testing aspheric surfaces. In addition, methods using heterodyne techniques and real time holography will be described.

Introduction

Although basic interferometry and holographic interferometry have not changed much during the last decade, the use of electronic solid state detector arrays, microprocessors, and computers for extracting information from the interferograms is becoming more common and sophisticated. The techniques become very useful for industrial applications, for contactless surface and deformation measurement as well as for strain, displacement, and vibration analysis and flow measurements. Heterodyne interferometry is one of the interferometric measuring techniques which make use of a reference beam shift or modulation to get high precision.

In optical testing computer analysis is becoming increasingly important. Much more information can be extracted from the interferograms leading to higher sensitivities. The application of holographic interferometry and speckle methods in real time leads to more appropriate techniques for engineering applications. Thermoplastic material is used frequently today. Photorefractive crystals are found to be useful for real time holography and speckle applications.

Interferometric testing

Solid state detector arrays, and microprocessors are mostly responsible for the progress in interferometric testing being made during the last few years. Digital interferometry provides a means of obtaining very precise measurements at rapid rates.

For the fringe analysis many different methods are applied. They can be classified into static and dynamic methods. In static methods a tilt is introduced to avoid closed fringes. The fringe centers can be found manually and by using a digitizing tablet as well as by using video- and image processing techniques. Furthermore, phase detection technique in the spatial domain using Fourier transformation¹ or Fourier analysis in connection with video technique can be used.

For dynamic algorithms the relative phase of the reference beam and the test beam in an interferometer is varied at constant, controlled rate or in steps of 90 or 120 degrees for instance.² The intensity of the interference pattern can be written as

$$I(x,y) = a(x,y) + b(x,y) \cos[\phi(x,y) + \Delta]$$

where $\phi(x,y) = \frac{2\pi}{\lambda} W(x,y)$ is the phase distribution of the wavefront $W(x,y)$ across the interference pattern to be measured and Δ the deliberately introduced phase shift. The interference pattern can be recorded by a solid state detector array. At least three fringe patterns with the appropriate phase shifts need to be recorded. The intensity measurement with phase changes of 90 degrees can be written

$$I_1(x,y) = a(x,y) + b(x,y) \cos[\phi(x,y)]$$

$$I_2(x,y) = a(x,y) + b(x,y) \cos[\phi(x,y) + \pi/2]$$

$$I_3(x,y) = a(x,y) + b(x,y) \cos[\phi(x,y) + \pi]$$

leading to the phase distribution across the fringe pattern, namely

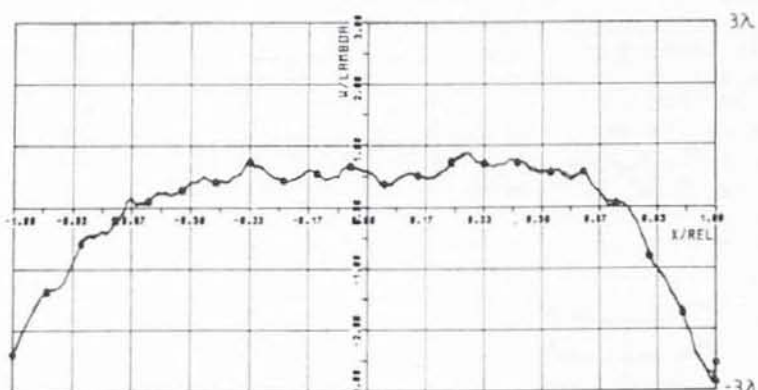
$$\phi(x,y) = \tan^{-1} \frac{2I_2(x,y) - I_1(x,y) - I_3(x,y)}{I_3(x,y) - I_1(x,y)}$$

Digital interferometry is very useful for getting the interferometric data into a computer for the analysis. Computer analysis of interferometric data can be carried out in different ways leading to precise measurements for testing wavefronts of optical surfaces and components. A fringe pattern of a deformed spherical Germanium surface obtained with a Twyman-Green interference arrangement is shown in Figure 1a. The experimental arrangement is shown in Figure 2 without the CGH and the lenses L_1, L_2, L_3 but L'_1 . For the automatic fringe analysis of closed fringes a plane-parallel plate is tilted in the reference beam to introduce phase shifts of 90 degrees. A one-dimensional fringe analysis is shown in Figure 1b., the corresponding one-dimensional "microstructure" analysis obtained from the same interference pattern is shown in Figure 1c. The sensitivity obtained is $\lambda/100$. For the



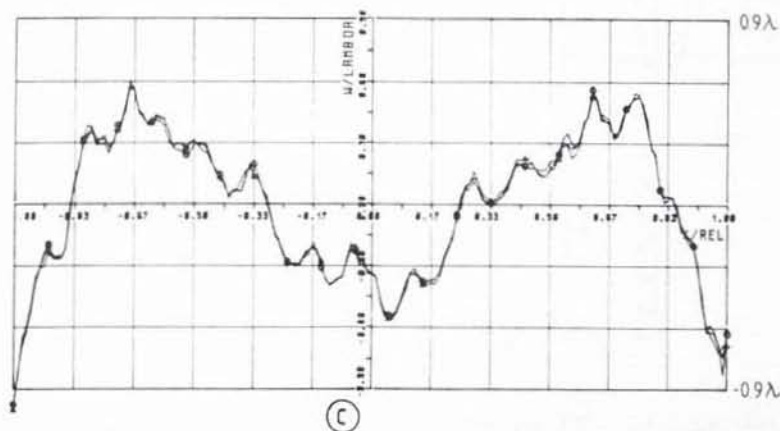
(a)

Figure 1a. Interference pattern obtained from a spherical diamond turned spherical surface tested with $\lambda = 633$ nm.



(b)

Figure 1b. One-dimensional fringe analysis of Fig. 1a using 2048 data points.



(c)

Figure 1c. Microstructure analysis of Fig. 1a.

automatic fringe analysis a Fairchild CCD line scan camera with 2048 elements together with an IBM PC was used. Alternatively for one- and two-dimensional analysis we very often use a Hamamatsu C 1000 camera. From the fringe pattern stored in a small computer the desired information such as the aberration coefficients as well as the optical transfer function can be obtained. Zernike polynomials are found to be appropriate because of their orthogonal properties.³

For microprofile measurements, stylus instruments are among the most highly developed means of profiling of precision surfaces. Electron microscopy can be used to produce contour maps and surface profiles of precision surfaces by using two perspective angles.

Interferometric techniques are well suited for microprofile measurements. Two as well as multiple beam interference arrangements with an automated fringe analysis can lead to a re-

solution of the order of 1 \AA as shown by Wyant and coworker.⁴ Recently heterodyne interference arrangements were presented capable of $0,1 \text{ \AA}$ vertical resolution and a few micrometer lateral resolution.⁵

Application of computer generated holograms for testing aspheric surfaces

Aspheric surfaces can be tested by a point analysis together with a 3-dimensional measuring device to generate the surface profile. Interferometric methods such as null test methods or shearing techniques as well as the application of holographic techniques and computer generated holograms are very useful for high precision measurements.

Computer generated holograms (CGH) can be used to compensate or compare complicated wavefronts for different applications. The CGH in a Twyman-Green experimental arrangement as shown in Figure 2. can be used to compensate the aspheric wavefront reflected by the lens under test, for instance. Illuminating the CGH with the perfect aspheric wavefront computed from the optical data leads, after diffraction, to a perfect plane wave to be compared with the perfect reference plane wave from the reference beam reflected from mirror MS. The interference fringes to be analysed are a measure of the discrepancy from the data of the aspheric component or surface. Alternatively, an aspheric wave front can be reconstructed from the CGH to be compared with the actual wavefront.

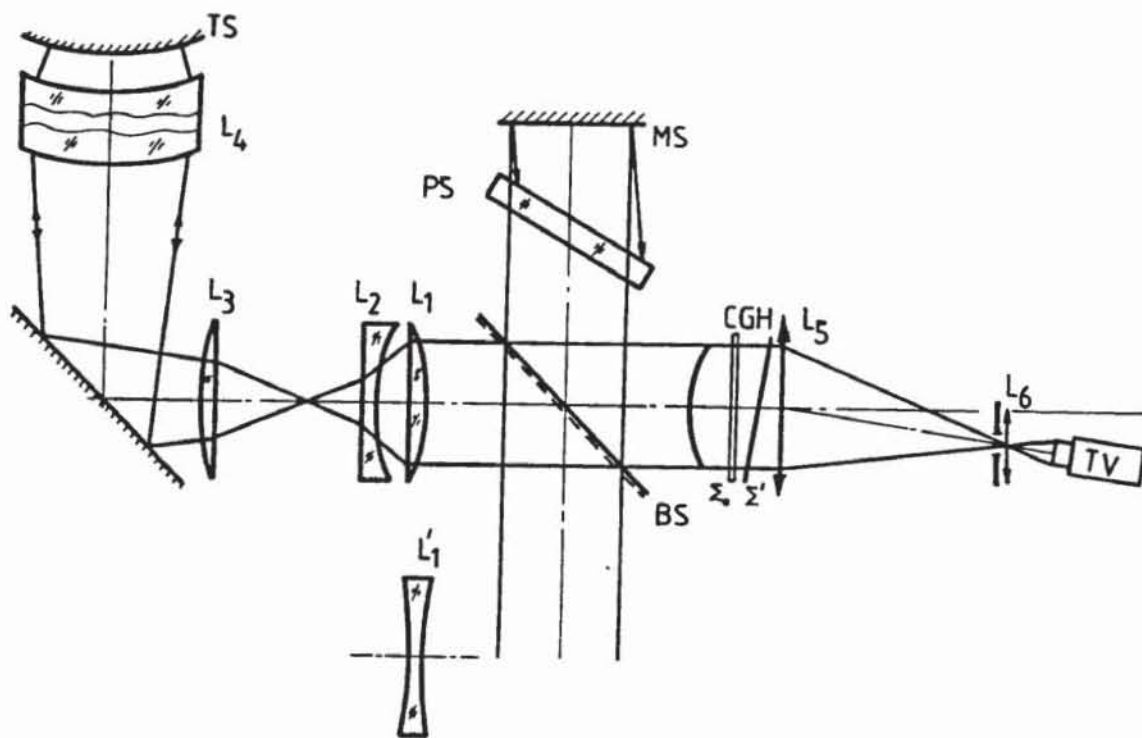


Figure 2. Experimental set-up for testing spherical and aspherical surfaces. BS = beam splitter, MS = reference mirror, L_1, L_2, L_3 = auxiliary lenses, PS = plane-parallel plate for phase shifting the reference beam, L_4 = high quality lens for testing spherical as well as aspherical surfaces, L'_1 = auxiliary lens to be used together with L_4 for testing spherical surfaces as well as for determining the vertex of the aspheric test lens accurately.

The principle of CGH is not new. Wyant among others described the technique in chapter 13 of Reference 2. It's application for the accurate, absolute test of steep aspheric surfaces as well as the generating of CGH needed to be improved.⁶

To generate the CGH different techniques have been devised or are in the process of being developed such as the use of electron beam scanners. We apply a computer driven Optronics drum scanner. A two beam interference arrangement for an off-axis hologram for testing aspheric surfaces is shown in Figure 2. The incident wave is separated by the beam splitter into the reference beam reflected back from the mirror MS slightly obliquely and passing through the hologram undisturbed and the test beam. For the fringe analysis of closed fringes a plane-parallel plate is used to shift the phase by steps of $\pi/2$. The simple lenses

L_1, L_2, L_3 are auxiliary lenses to adapt the aperture of the lens under test TS. They should also image the test surface onto the CGH, a necessary condition for strong aspheric wavefronts. Furthermore they can also be used to compensate some of the aspheric wavefront. L_4 is a high quality lens to be used for testing aspherical as well as spherical lenses without a CGH by replacing the auxiliary lenses by L_1 . In addition L_4 and L_1 are used for focussing on the surface under test as well as for testing spherical surfaces with the same instrument. Furthermore, the accurate position of the vertex for spherical and aspherical surfaces is obtained with L_1 in place.

Although the auxiliary lenses need not be perfect a hologram is computed at first for a known spherical surface; the fringe analysis leads to a compensation of the errors involved which in turn are compensated when computing the CGH for the test surface.

Adjustment in an industrial test procedure can be time consuming and difficult because 7 degrees of freedom need to be balanced such as tilt and decentring in two directions of the test surface as well as decentring and rotation of the hologram; some of the adjustment errors have similar effects on the interference pattern.

Using the previously described automatic fringe analysis it was found appropriate to approximate the measured wavefront $W(r, \theta)$ by a set of polynomials. Zernike polynomials were used because of their orthogonal properties. They lead to an elimination of the influence of the actual adjustment errors by matching the ray tracing program and the measured wavefront.

The approximation of the measured wavefront $W(r, \theta)$ can be written

$$W(r, \theta) \cong w(r, \theta) = \sum_{j=0}^N A_j U_j(r, \theta)$$

$$\text{where } U_j(r, \theta) = R_n^m(r) \begin{cases} \sin m\theta & \text{for } m < 0 \\ \cos m\theta & \text{for } m > 0 \end{cases}$$

are Zernike polynomials of order n and azimuth frequency m . Taking into account that mainly odd terms arise when decentring and tilting the optical elements by a small amount, only polynomials with $m = \pm 1$ need to be evaluated whereas symmetrical errors such as defocus and errors in the vertex radius are described by $m = 0$.

Calculating the derivatives of the Zernike coefficients $A_2 \dots A_{33}$ of the wavefront computed by ray tracing with respect to tilt β and decentring ϵ of the aspheric surface and the hologram a set of linear equations is obtained.

For

$$\begin{bmatrix} A_2 \\ \cdot \\ \cdot \\ A_{33} \end{bmatrix} = \begin{bmatrix} \frac{\partial A_2}{\partial \beta_{Rx}} & \frac{\partial A_2}{\partial \beta_{Ry}} & \dots & \frac{\partial A_2}{\partial \epsilon_{Hx}} & \frac{\partial A_2}{\partial \epsilon_{Hy}} \\ \cdot & \cdot & \cdot & \cdot & \cdot \\ \cdot & \cdot & \cdot & \cdot & \cdot \\ \frac{\partial A_{33}}{\partial \beta_{Rx}} & \frac{\partial A_{33}}{\partial \beta_{Ry}} & \dots & \frac{\partial A_{33}}{\partial \epsilon_{Hx}} & \frac{\partial A_{33}}{\partial \epsilon_{Hy}} \end{bmatrix} \begin{bmatrix} \beta_{Rx} \\ \beta_{Ry} \\ \epsilon_{Ax} \\ \epsilon_{Ay} \\ \beta_{Ax} \\ \beta_{Ay} \\ \epsilon_{Hx} \\ \epsilon_{Hy} \end{bmatrix}$$

To obtain tilts β and decentring of the measured fringe pattern the above equation needs to be inverted. Linearity can be assumed for small adjustment errors; for stronger errors an iterative process like the damped least square method can be applied.

Once the adjustment errors have been calculated, their contribution to the wavefront can easily be determined in terms of Zernike polynomials, which in turn need to be subtracted from the measured wavefront. Typical results are shown in Figure 3, where different centring errors needed to be found from four interferograms. Only two fringe patterns with centring errors $\epsilon = 0,01$ mm and $\epsilon = 0,10$ mm are shown in Figure 3a. After the centring error was found from the interferogram or wavefront in Figure 3b, it was subtracted to lead to the wavefront in Figure 3c. The same procedure was applied for a more complicated fringe pattern in Figure 4, with centring errors, tilt of the aspherical surface as well as decentring of the CGH for the same test as in Figure 3. After determining the adjustment errors from the fringe pattern and subtracting the wavefront from adjustment errors an almost perfect agreement with Figure 3c was obtained. Further investigations are, however, needed. For high precision measurements the automatic fringe analysis together with a compensation of adjustment errors will become useful for industrial applications.

COMPENSATION OF DECENTERING OF ASPHERIC SURFACE

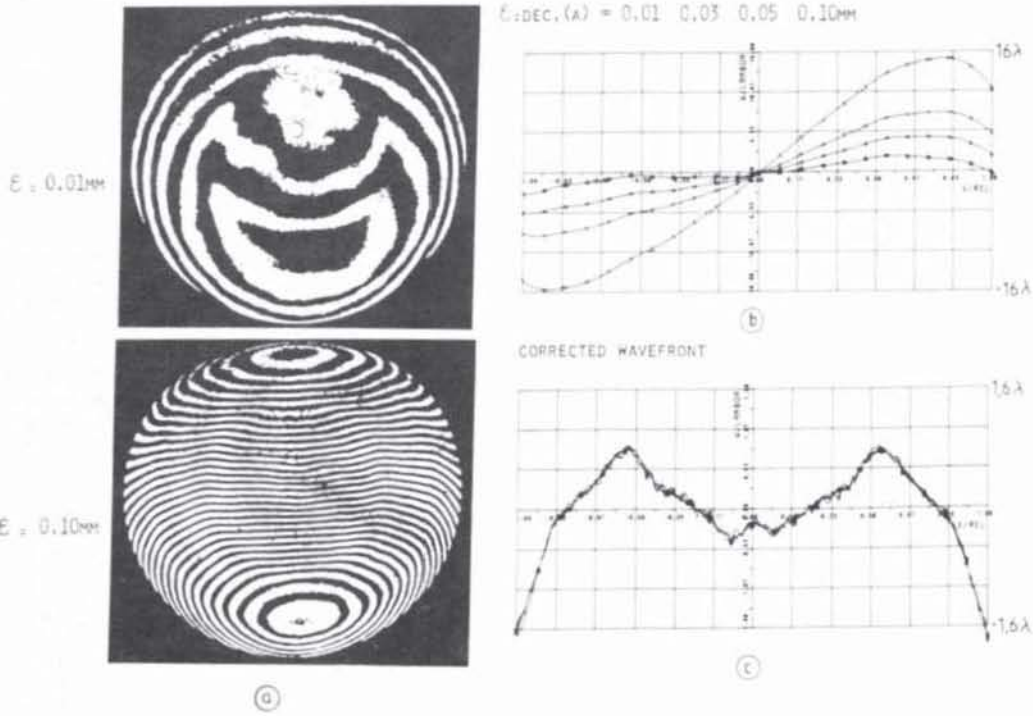


Figure 3.

COMPENSATION OF ADJUSTMENT ERRORS

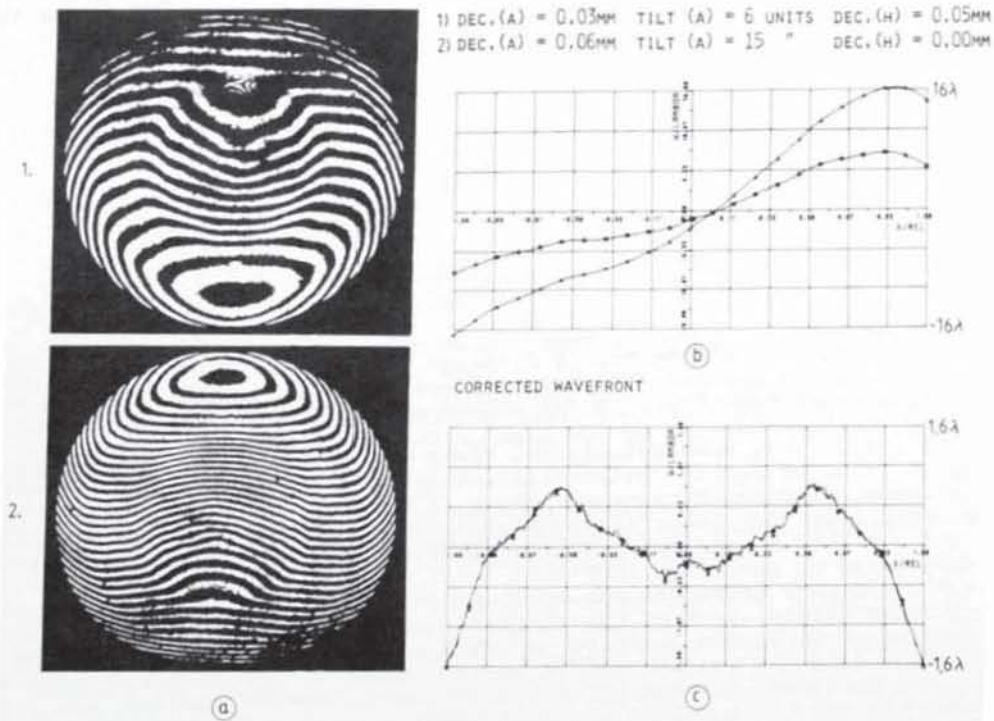


Figure 4.

Application of heterodyne interferometry

Figure 5. shows schematically an arrangement for heterodyne interferometry. In classical interferometry, phase differences of optical fields are transformed into detectable intensity variations. In two beam heterodyne interferometry the two light fields are assumed to be

$$A_1 = a_1 \cos(\omega_1 t + \phi_1)$$

and

$$A_2 = a_2 \cos[\omega_1 t + \Delta\omega t + \phi_2 + \phi(t)]$$

where $\Delta\omega$ is the ^{ang} frequency shift which can be introduced by a Bragg cell or a moving grating. In heterodyne detection by a square-law detector the detector output is

$$I = 2a_1 a_2 \cos(\Delta\omega t + \phi(t) + \phi_2 - \phi_1)$$

where the time varying phase variation $\phi(t)$ can be detected. The measurement of the velocity v (parallel to the optical axis in Figure 5. follows from $\phi(t) = \frac{2\pi}{\lambda} 2v(t) \cdot t$

For a harmonically oscillating object $\phi(t) = \frac{4\pi}{\lambda} \rho \cos \Omega t$ producing a frequency modulated output signal at the detector with a carrier frequency of $\Delta\omega$ and a frequency modulation of Ω and ρ the amplitude of oscillation. The signal can be evaluated by well known frequency analysis techniques. The microprofile of Figure 6. was obtained by scanning a surface with a heterodyne interference arrangement similar to Figure 5. The resolution obtained so far is a few Å.

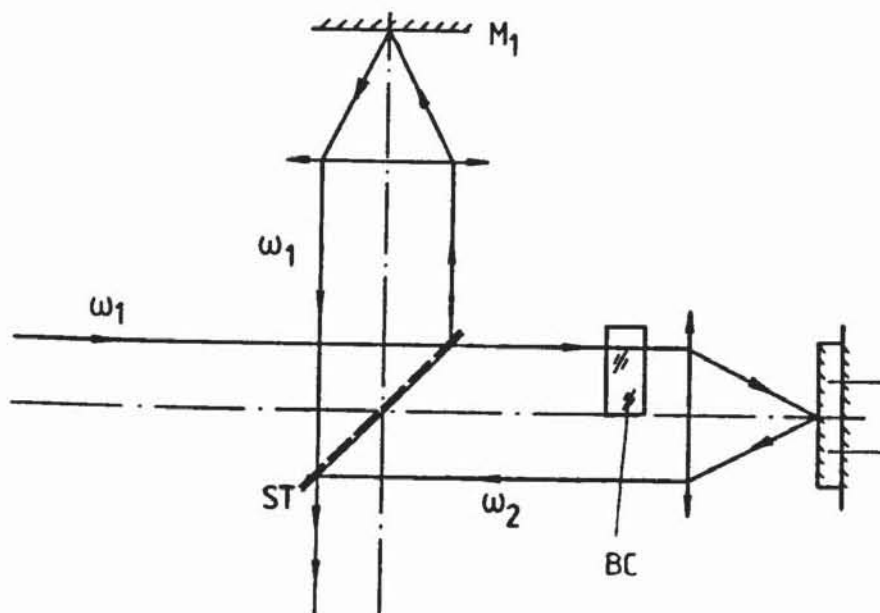


Figure 5. Principle of a heterodyne arrangement.

Figure 7. shows an example of the frequency analysis leading to the velocity at a single point (perpendicular to the surface) of the side wall of a rotating car-tyre obtained with heterodyne interferometry. The arrangement used is shown schematically in Figure 5. For comparison an independent measurement obtained by a microphone is indicated by dotted lines in Figure 7. Close agreement is obtained between the noise detected with a microphone and the noise generated by vibration only.

Heterodyne interferometry will lead to very useful future applications in precision measurements. For the vibration analysis at given points heterodyne interferometry gives not only the amplitude of vibration parallel to the line of sight but also the frequency. Furthermore, it helps for the fringe analysis in holographic interferometry when it is used to relate the fringes to a known amplitude of vibration obtained by a heterodyne technique.

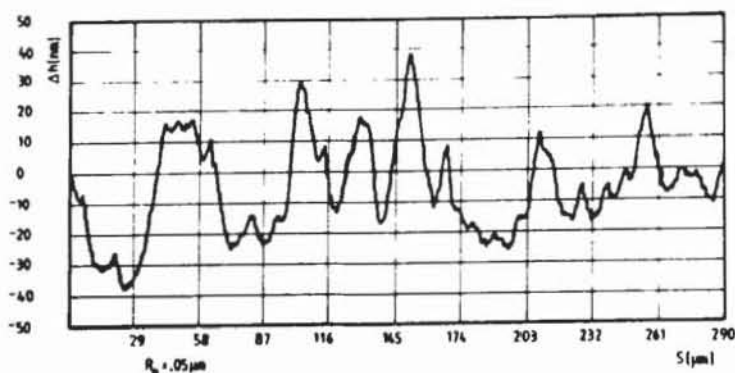


Figure 6. Microprofile obtained with heterodyne interferometry.

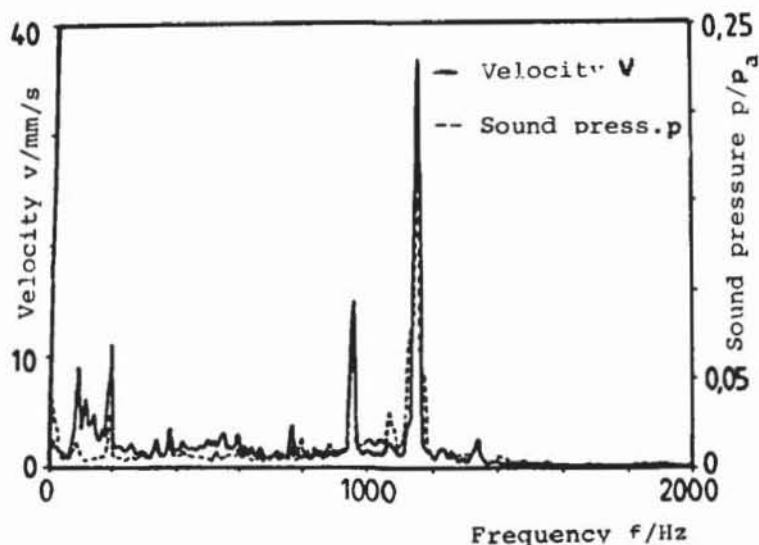


Figure 7. Comparison of the vibration analysis of a rotating car-tyre using heterodyne interferometry and with a microphone placed appropriately.

Holographic interferometry in real time

Holographic interferometry has now progressed to a point where the analysis of the fringe patterns together with extracting the required information needs to be improved further. Heterodyne interferometry and holographic interferometry leads to the information of amplitude and frequency of the object movement at given points. For rotating objects, the unwanted rigid body rotation needs to be eliminated while preserving the information about the elastic subject deformation. Image derotation is the most promising approach for the study of rotating objects with holographic or speckle techniques. In image-derotated holographic interferometry the image of the rotating object is passed through, or reflected by, a prism rotating at half rotational speed of the object, thus cancelling out the rotational motion. A Q-switch double-pulsed ruby laser can be used to produce a double-exposure hologram of the rotating object; examples of fringe pattern of a rotating car-tyre by road contact will be shown.

Holographic interferometry is more attractive for the engineer when it can be applied in real time. Photothermoplastic material is frequently used as storage material⁵ by now. Photorefractive crystals can be applied for real time metrology using holography⁵ in a two or four wave mixing arrangement or speckle techniques. The $\text{Bi}_{12}\text{SiO}_{20}$ photorefractive crystal is a very promising storage material to be applied for real time holography and speckle applications.^{8,9} The sensitivity can be improved by energy transfer from pump reference beam to the low intensity signal beam¹⁰ leading to new applications in optical metrology.¹¹

References

1. Takeda, M., Ina, H. and Kobayashi, S., "Fourier transform method for fringe pattern analysis for computer-based topography and interferometry", *JOSA* 72, pp 156-160. 1982.
2. Wyant, J. C., Chapter 12 in *optical shop testing*, ed. Malacara, D., John Wiley and Sons, New York 1978.
3. Küchel, F. M., Schmieder, Th. and Tiziani, H. J., "Beitrag zur Verwendung von Zernike-Polynomen bei der automatischen Interferenzstreifenwertung", *Optik* 65, pp. 123-142. 1983.
4. Wyant, J.C., Koliopoulos, C. L. and Bhusban, B., *ASCE Transaction* 27, pp.101. 1984.
5. Huang, C. C., "Optical heterodyne profilometer", *Optical Engineering*, Vol. 23, pp. 365-370. 1984.
6. Dörband, B., Tiziani, H. J., "Auslegung von Kompensationssystemen zur interferometrischen Prüfung asphärischer Flächen", *Optik* 67, pp. 1-20. 1984.
7. Dändliker, R., *Progress in Optics*, ed. Wolf, E., North Holland Publ., Amsterdam 1980. Vol. XVII, 1.
8. Huignard, J. P., Herriau, J.P., Aubourgh, P. and Spitz, E., "Phase-conjugate wavefront generation via real-time holography in $\text{Bi}_{12}\text{SiO}_{20}$ crystals", *Opt. Lett.* 4, pp. 21. 1979.
9. Tiziani, H. J., "Realtime metrology with BSO crystals", *Optica Acta*, Vol. 29, pp. 463-470. 1982.
10. Rajbenbach, H., Huignard, J. F. and Loisseaux, B., "Spatial Frequency Dependence of the Energy Transfer in Two-Wave Mixing Experiments with BSO crystals", *Opt. Comm.* 48, pp. 247. 1983.
11. Küchel, F. M., Tizani, H. J., "Real-time contour holography using BSO-crystals", *Opt. Comm.* 38, pp.17. 1981.